








Whole cell melanoma vaccine genetically modified to stem cells like phenotype generates specific immune responses to ALDH1A1 and long-term survival in advanced melanoma patients

Eliza Kwiatkowska-Borowczyk ^{a,b}, Patrycja Czerwińska ^{a,b}, Jacek Mackiewicz^{b,c}, Katarzyna Gryśka^a, Urszula Kazimierzczak^a, Katarzyna Tomela ^a, Anna Przybyła^a, Anna Karolina Kozłowska ^a, Łukasz Galus^{c,d}, Łukasz Kwinta^d, Ewelina Dondajewska ^a, Agnieszka Gąbka-Buszek^a, Monika Żakowska ^a, and Andrzej Mackiewicz ^{a,b}

^aChair of Medical Biotechnology, Poznan University of Medical Sciences, Poznan, Poland; ^bDepartment of Diagnostics and Cancer Immunology, Greater Poland Cancer Centre, Poznan, Poland; ^cDepartment of Medical and Experimental Oncology, Heliodor Swiecicki University Hospital, Poznan University of Medical Sciences, Poznan, Poland; ^dDepartment of Chemotherapy, Greater Poland Cancer Centre, Poznan, Poland

ABSTRACT

Allogeneic whole cell gene modified therapeutic melanoma vaccine (AGI-101H) comprising of two melanoma cell lines transduced with cDNA encoding fusion protein composed of IL-6 linked with the soluble IL-6 receptor (sIL-6R), referred to as H6 was developed. H6 served as a molecular adjuvant, however, it has altered vaccine cells phenotype towards melanoma stem cells (MSC)-like with high activity of aldehyde dehydrogenase isoenzyme (ALDH1A1). AGI-101H was applied in advanced melanoma patients with non-resected and resected disease. In the adjuvant setting, it was combined with surgery in case of recurring metastases, which were surgically removed and vaccination continued. A significant fraction of AGI-101H treated melanoma patients is still alive (11–19 years). Out of 106 living patients, 39 were HLA-A2 positive and were the subject of the study. Immunization of melanoma patients resulted in the generation of cytotoxic CD8⁺ T cells specific for ALDH1A1, which were detected in circulation by HLA-A0201 MHC dextramers loaded with ALDH1A1₈₈₋₉₆(LLYKLADLI) peptide. Phenotypically they were central memory CD8⁺ T cells. Re-stimulation with ALDH1A1₈₈₋₉₆ *ex vivo* resulted in IFN- γ secretion and cells degranulation. Following each vaccine dose administration, the number of ALDH1A1-CD8⁺ T cells increased in circulation and returned to the previous level until next dose injection (one month). ALDH1A1-CD8⁺ T cells were also found, however in the lower number than in vaccinated patients, in the circulation of untreated melanoma with stage IV but were not found in stage II or III and healthy donors. Specific anti-ALDH1 antibodies were present in treated patients. Long-term survival suggests immuno-targeting of MSC in treated patients.

ARTICLE HISTORY

Received 7 May 2018
Revised 2 August 2018
Accepted 4 August 2018

KEYWORDS

Melanoma; whole cell melanoma vaccine; ALDH1A1; melanoma stem cells; immunotargeting; IL-6 transsignaling; Hyper-IL6

Introduction

Surgery of the thin primary skin melanoma is curable in the significant number of patients; however advanced metastatic melanoma is still a deadly disease. Recent developments in targeted and immune-therapies such as immune checkpoint inhibitors led to the statistically significant extension of overall survival (OS) of a fraction of metastatic melanoma patients. However, the clinical benefits were often transient and associated with serious adverse events.¹

Tumors formed by transformed cells, due to the developing hypoxia, create local microenvironment, which induces neo-angiogenesis, changes the metabolism of cancer cells, expression of checkpoint molecules, what leads to local tumor immune-suppression.² An important role in cancer progression plays a small fraction of cells referred to as cancer-initiating or cancer stem cells (CSC).³ Melanoma appears to be the tumor with the relatively high frequency of CSC (up to 27%). CSCs are self-renewing, multi-differentiating, and are involved in local tumor

recurrence and distant metastases. CSCs are resistant to conventional therapies such as chemo- or radiotherapy. Accordingly, they are the targets for novel therapeutic strategies.⁴

We have developed allogeneic whole cell gene modified therapeutic melanoma vaccine (AGI-101H) comprising of two melanoma cell lines. The vaccine cells were virally transduced with a designer cytokine gene encoding fusion protein comprising interleukin 6 (IL-6) linked with the soluble IL-6 receptor (sIL-6R), referred to as Hyper-IL-6 or H6.^{5,6} The H6 serves as a molecular adjuvant, however, on the autocrine manner, it has altered vaccine cells phenotype towards melanoma stem cells (MSC)-like with high activity of aldehyde dehydrogenase isoenzyme (ALDH1A1).^{6,7}

AGI-101H was applied in advanced melanoma patients with non-resected and resected metastases.^{8,9} In patients with resected metastases vaccination was combined with surgery of recurring metastases, which were surgically removed, and vaccination continued. A significant fraction

of AGI-101H treated melanoma patients is still alive (from 11 to 19 years) and are the subjects of the study. Out of 106 living patients, 39 were HLA-A2 positive. In all these patients, cytotoxic CD8⁺ T cells (CTL) specific for ALDH1A1, which were functionally active were detected in circulation. Following each vaccine administration, the number of specific CTL increased and returned to the previous level at the time of the next boosting dose injection (one-month interval). In addition, immunization with AGI-101H increased anti-ALDH1 antibodies production.

Results

H6 induces STAT3 phosphorylation in vaccine cells

Both tyrosine 705 and serine 727 residues of STAT3 in H6 modified Mich1 and Mich2 vaccine cells were phosphorylated (Figure 1A). In Mich1H6 cells, the MFI for STAT3 pY705 increased from 33.2 to 48.1 (1.5-fold) and the MFI for STAT3 pS727 from 98.6 to 116 (1.2-fold). In Mich2H6 cells, the MFI for STAT3 pY705 increased from 25.6 to 47.4 (1.9-fold) and the MFI for STAT3 pS727 from 89.5 to 158 (1.8-fold).

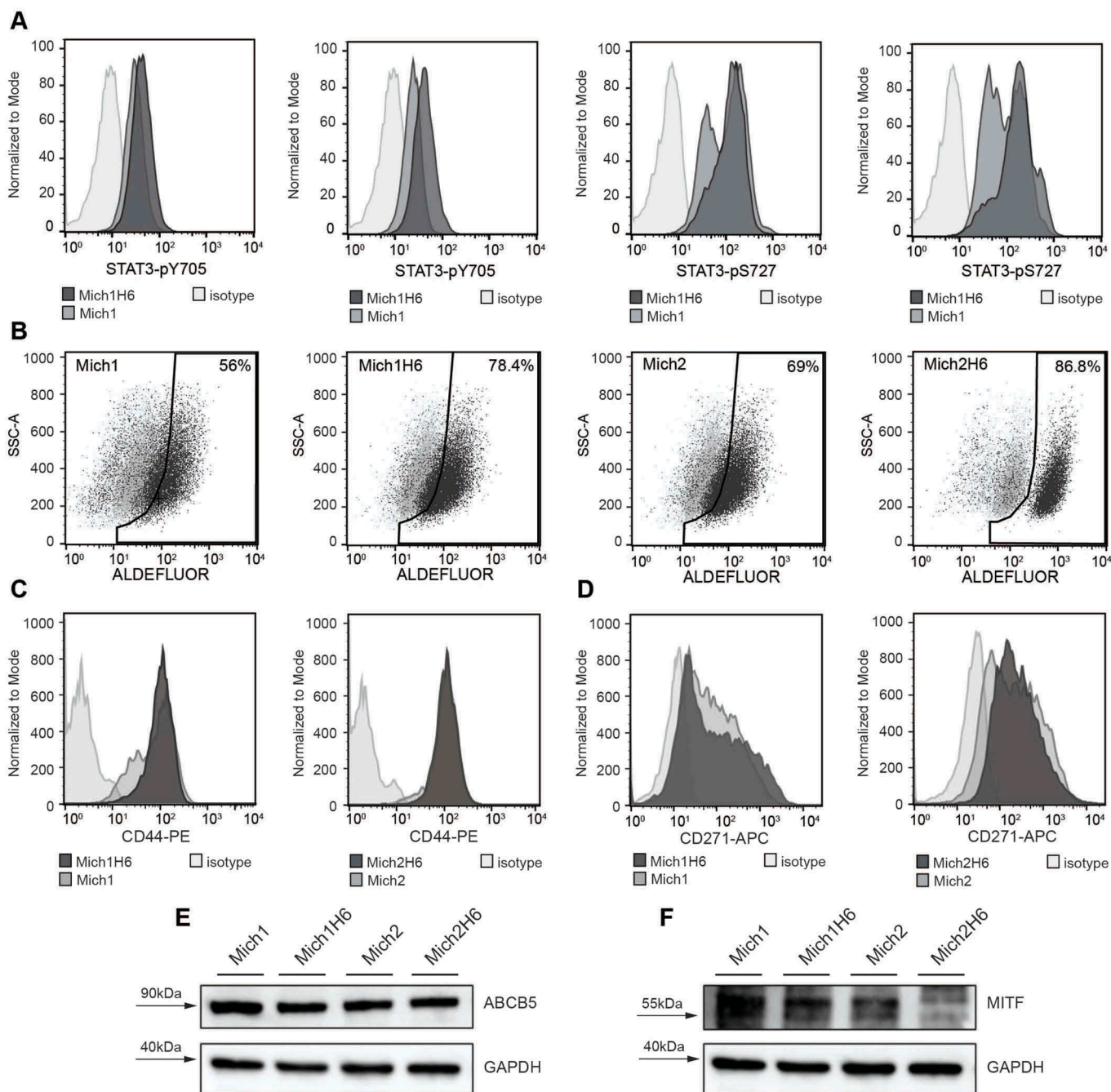


Figure 1. H6 upregulates phosphorylation of STAT3 transcription factor in AGI-101H cell lines Mich1 and Mich2 that elicit expression of melanoma-initiating cell markers ALDH1, CD271, ABCB5, as well as a microphthalmia-associated transcription factor (MITF). A. Flow cytometry analysis of STAT3-pY705 and STAT3-pS727 modifications in Mich1 and Mich2 cell lines as well as their Hyper-IL6-modified derivatives. B. Flow cytometry analysis of ALDH1 activity demonstrated with Aldefluor assay. C and D. Flow cytometry analysis of CD44 (C) and CD271 (D) expression on the surface of Mich1 and Mich2 cell lines as well as their Hyper-IL6-modified derivatives. E. Western blot analysis of ABCB5 marker. F. Western blot analysis of MITF. For Western Blot assays, GAPDH was used as an internal control.

AGI-101H vaccine cells exhibit the characteristics of melanoma-initiating cells like- phenotype

The stem cells like-phenotype of AGI-101H was analyzed by assessing the activity of ALDH1A1 and expression of CD271, ABCB5, CD44, and MITF. Both Mich1H6 and Mich2H6 cells showed higher ALDH1A1 activity comparing to unmodified cells (56% vs 78,4% and 69% vs 86,8%, respectively (Figure 1B)). The H6 modification did not affect the expression of CD44, which was observed in all studied cell lines (Figure 1C). However, H6 augmented CD271 expression by a 2-fold increase of MFI in Mich1H6 cells (Figure 1D). Moreover, no differences in the ABCB5 levels in AGI-101H cell lines regardless of H6 modification were observed (Figure 1E). However, reduced MITF levels in the Mich2H6 as compared to unmodified cells were seen (35% signal reduction, Figure 1F).

In addition, expression of regulatory immune checkpoints such as PD-1 and PD-L1 was analyzed in AGI-101H cells, which revealed weak expression of PD-L1 molecules on vaccine cells (data not shown).

Vaccination with AGI-101H leads to expansion of ALDH1A1-specific CD8+ T cells in treated patients

The frequency of ALDH1A1-specific CD8⁺ T cells was analyzed before the subsequent vaccine dose administration

(day 0) and 6 days after that. Such procedure was repeated a few times during the treatment. The gating strategy for analysis of ALDH1A1-specific CD8⁺ T cells was presented in Supplemental Figure 1A. ALDH1A1-specific CD8⁺ T cells in all patients enrolled in the study were found (Figure 2). Representative results are presented in Figure 2A. The frequency ranged between 0.001 and 0.67% at day 0, with mean 0.1% (median 0.05%). In 28 patients tested (72%) increased frequencies of ALDH1A1-specific CD8⁺ T cells 6 days following vaccine administration (range 0.02–0.74%; mean 0.17%; median 0.12%) were observed. The increase ranged from 1.25 to 53 (mean 7.63; median 2.84) folds ($p < 0.0001$, Figure 2B).

In 21 patients (88%) of not AGI-101H treated HLA-A2 control melanoma patients the ALDH1A1-specific CD8⁺ T cells were also found. The overall range was 0–0.29% (mean 0.06%; median 0.02%) and it was significantly lower than in patients 6 days following vaccine administration ($p < 0.0001$, Figure 2C). Due to the disease stage heterogeneity, the control group was divided into two subgroups, stage II-IIIc (7 patients) and stage IV (14 patients). The range of ALDH1A1-specific CD8⁺ T cells in stage II-IIIc group was 0% to 0.1% (mean 0.02%; median 0.01%), and the frequency was significantly lower than in patients enrolled into the AGI-101H clinical trials, irrespectively of

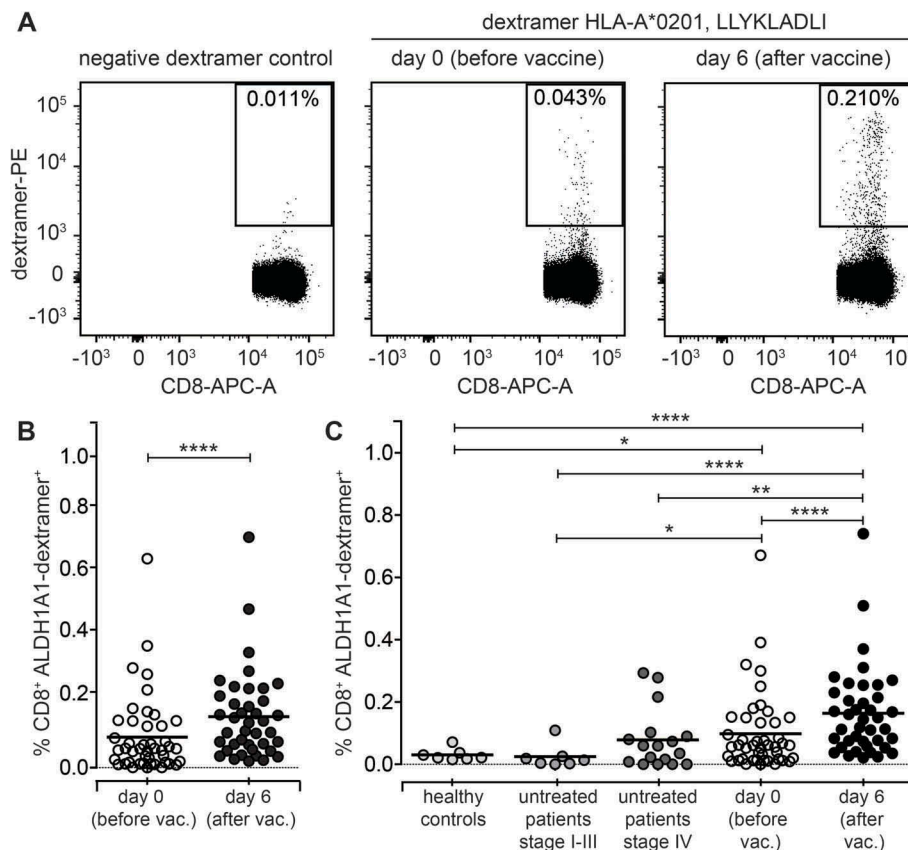


Figure 2. Immunization with AGI-101H significantly increases the frequency of ALDH1-specific CD8⁺ T cells. A. Representative analysis of ALDH1-specific CD8⁺ T cells in melanoma patient immunized with the AGI-101H vaccine. B. Cytometric data of multiparametric analysis of the frequency of ALDH1-specific CD8⁺ T cells performed before and after administration of single dose of AGI-101H vaccine were statistically analyzed using Wilcoxon matched-pairs signed rank test. **** $p < 0.0001$. Data are presented as dot plots with mean shown as a line. C. Cytometric data obtained for healthy controls ($n = 10$), untreated patients divided into patients with stage II-III ($n = 7$), AGI-101H-vaccinated patients ($n = 39$) at day 0 and at day 6, were statistically analyzed using Kruskal-Wallis test, $p < 0.0001$. Differences between groups were tested using Mann Whitney U test. **** $p < 0.0001$, *** $p = 0.002$, ** $p = 0.007$, * $p = 0.03$. Data are presented as dot plots with mean shown as a line.

the time point ($p = 0.029$ for day 0, $p < 0.001$ for day 6). In stage IV control group the range was 0% to 0.29% (mean 0.08%; median 0.06%) and it was significantly lower than in treated patients at day 6 ($p = 0.007$). The frequencies of ALDH1A1-specific CD8⁺ T cells in healthy controls were similar to the untreated patients with stage II-IIIc, with range 0.002–0.05% (mean 0.02%; median 0.02%). It was significantly lower than in HLA-A2 long-term survivors, both at day 0 ($p = 0.03$) and 6 days following vaccine administration ($p < 0.0001$; [Figure 2C](#)).

ALDH1A1-specific CD8⁺ T cells acquire central memory phenotype

To determine the differentiation phenotype of ALDH1A1-specific CD8⁺ T cells, untouched CD8⁺ T cells from AGI-101H treated melanoma patients were separated with magnetic beads and further subjected for immunostaining with anti-CD45RA, anti-CCR7 and ALDH1A1-dextramer together with anti-CD8 and anti-CD3 antibodies. The gating strategy for phenotypic analysis of ALDH1A1-specific CD8⁺ T cells was presented in [Supplemental Figure 1B](#). The purity of magnetic separation was very high with >80% of CD3⁺CD8⁺ T cells. Due to the ethical limits of the blood volume withdrawn from the study patients and relatively small populations of ALDH1A1-specific CD8⁺ T cells, PBMC were isolated only from 3 patients with a relatively high frequency of ALDH1A1-specific CD8⁺ T cells. Representative results of CD8⁺ T cell differentiation phenotyping of both ALDH1A1-specific CD8⁺ T cells and non-specific CD8⁺ T cells are presented in [Figure 3](#). The average frequency of ALDH1-specific CD8⁺ T cells with central memory phenotype (CD45RA-CCR7⁺) ranged from 10.75% ($\pm 0.55\%$) to 22.15% ($\pm 0.75\%$) at the day 0 and 6 days after vaccination, respectively ([Figure 3B](#)).

ALDH1A1-specific CD8⁺ T cells are functionally active

CD8⁺ T cells display two major effector functions: cytotoxic activity and cytokine production. Here we studied these functions by assessment of a granule-dependent (perforin/granzyme) pathway of antigen-specific CD8⁺ T cells using CD107a marker that is expressed on cell surface of these cells during degranulation and intercellular IFN- γ production. As previously, due to small populations of ALDH1-specific CD8⁺ T cells in patients enrolled to the study, only 3 patients with a high number of isolated PBMCs and relatively high frequency of ALDH1-specific CD8⁺ T cells were analyzed. The gating strategy for the analysis of functional activation of ALDH1A1-specific CD8⁺ T cells was presented in [Supplemental Figure 1C](#). AGI-101H-treated melanoma patients (at day 0 and six days after vaccine administration) were incubated with ALDH1A1₈₈₋₉₆ (LLYKLADLI) antigenic peptide and the expression of CD107a surface marker and IFN- γ production were analyzed. Stimulation with anti-CD3 and anti-CD28 antibodies as well as incubation with mixed Melanoma Associated Antigens (MAA; gp-100, NY-ESO and Tyrosinase peptides)

were used as positive controls of degranulation and IFN- γ production. The average frequencies of CD107a⁺IFN- γ ⁺ cells in ALDH1-stimulated CD8⁺ T cells at day 0 and 6 days after vaccination ranged from 1.48% ($\pm 1.18\%$) to 2.1% ($\pm 1.42\%$), respectively. This indicates functional activation of ALDH1A1-specific CD8⁺ T cells in AGI-101H-treated melanoma patients upon vaccine administration. We also observed enhanced activation of CD8⁺ T cells stimulated with mixed MAA peptides upon AGI-101H administration (CD8⁺CD107a⁺IFN- γ ⁺ cells at the day of vaccination: 1.85% ($\pm 1.38\%$), 6 days after vaccination: 4.77% ($\pm 3.92\%$)). Representative results of cytometric analyses are presented in [Figure 4](#).

AGI-101H treatment decreased the number of circulating myeloid-derived suppressor cells (MDSCs) in treated patients

We have also examined the impact of AGI-101H vaccination on the population of circulating Myeloid-Derived Suppressor Cells (MDSCs). MDSCs, characterized as CD57⁻CD11⁺CD14⁺HLA-DR⁻ cells, were analyzed by flow cytometry in 57 melanoma patients treated with AGI-101H (at the day of vaccine administration and 6 days later), 20 untreated melanoma patients and 14 healthy volunteers. The gating strategy for the analysis of MDSC cells was presented in [Supplemental Figure 1D](#). [Figure 5A](#) shows representative results of the MDSCs analysis in melanoma patient before and 6 days after vaccination, and in untreated controls. Statistical analysis of cytometric data revealed a significant increase in MDSCs in untreated melanoma patients compared to healthy controls, that is consistent with published data ([Figure 5B](#)). The mean percentage of CD57⁻CD11⁺CD14⁺HLA-DR⁻ in PBMCs was 0.45% for untreated melanoma patients and 0.003% for healthy volunteers ($p = 0.0001$). The median was 0.22% vs. 0.0027%, respectively. Immunization with AGI-101H resulted in a decrease of circulating MDSCs ([Figure 5B](#)). Percentage of CD57⁻CD11⁺CD14⁺HLA-DR⁻ in PBMCs measured on the day of vaccination (usually 4 weeks after previous vaccine dose) as well as 6 days after treatment, were significantly reduced compared to untreated patients ($p = 0.0001$).

Immunization with AGI-101H induces anti-ALDH1 antibodies

ALDH1 IgG response was analyzed in sera collected from 39 long-term survivors, 18 untreated patients, and 10 healthy controls. Antibody titers in AGI-101H treated patients were found in the range of 4,000–64,000 (median 16,000) dilution. They were significantly higher than the anti-ALDH1 IgG titers detected in untreated patients (range 2000–16000; median 8,000; $p = 0.037$, [Figure 6](#)). In healthy controls, the titer ranged from 2000 to 8000 (median 4,000) and was significantly lower than in both AGI-101H treated and untreated patients.

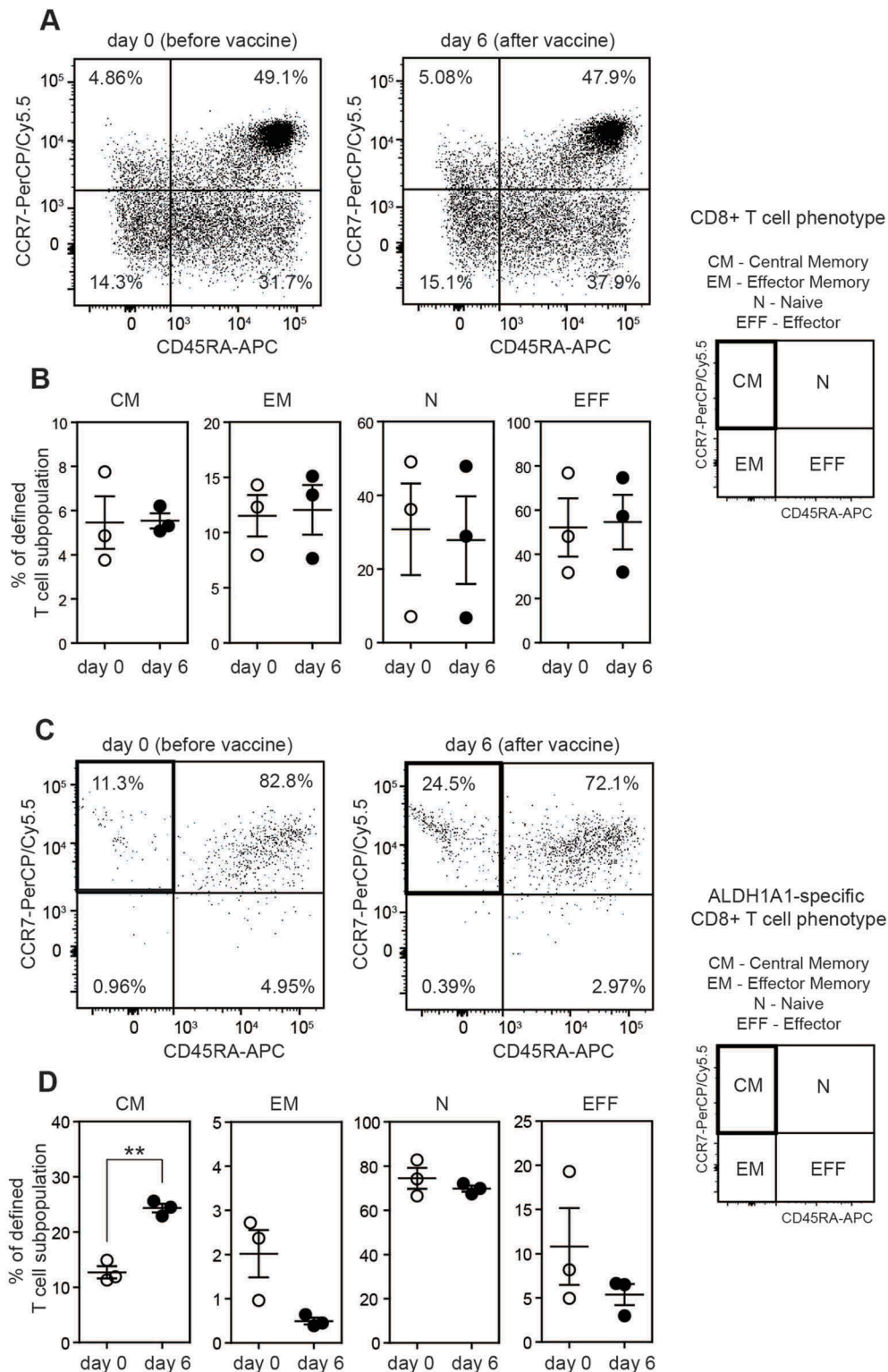


Figure 3. ALDH1A1-specific peripheral CD8+ T lymphocytes from vaccinated melanoma patients acquire Central Memory T cell phenotype (CM). **A.** Flow cytometry analysis of CD45RA and CCR7 cell surface markers on peripheral CD8+ T lymphocytes (not specific for ALDH1A1 (LLYKLADLI) peptide). Representative plots from AGI-101H vaccinated melanoma patient at day 0 and day 6 after vaccination are depicted. **B.** Percentage of defined peripheral CD8+ T cell subpopulations not specific for ALDH1A1 (LLYKLADLI) peptide in AGI-101H treated melanoma patients on the day of vaccine administration (day 0) and 6 days later. **C.** Flow cytometry analysis of CD45RA and CCR7 cell surface markers on peripheral CD8+ T lymphocytes specific for ALDH1A1 (LLYKLADLI) peptide. Representative plots from AGI-101H vaccinated melanoma patient at day 0 and day 6 after vaccination are depicted. **D.** Percentage of defined peripheral CD8+ T cell subpopulations specific for ALDH1A1 (LLYKLADLI) peptide in AGI-101H treated melanoma patients on the day of vaccine administration (day 0) and 6 days later. CM – Central Memory, EM – Effector Memory, N – Naive, EFF – Effector; ** $p < 0.005$.

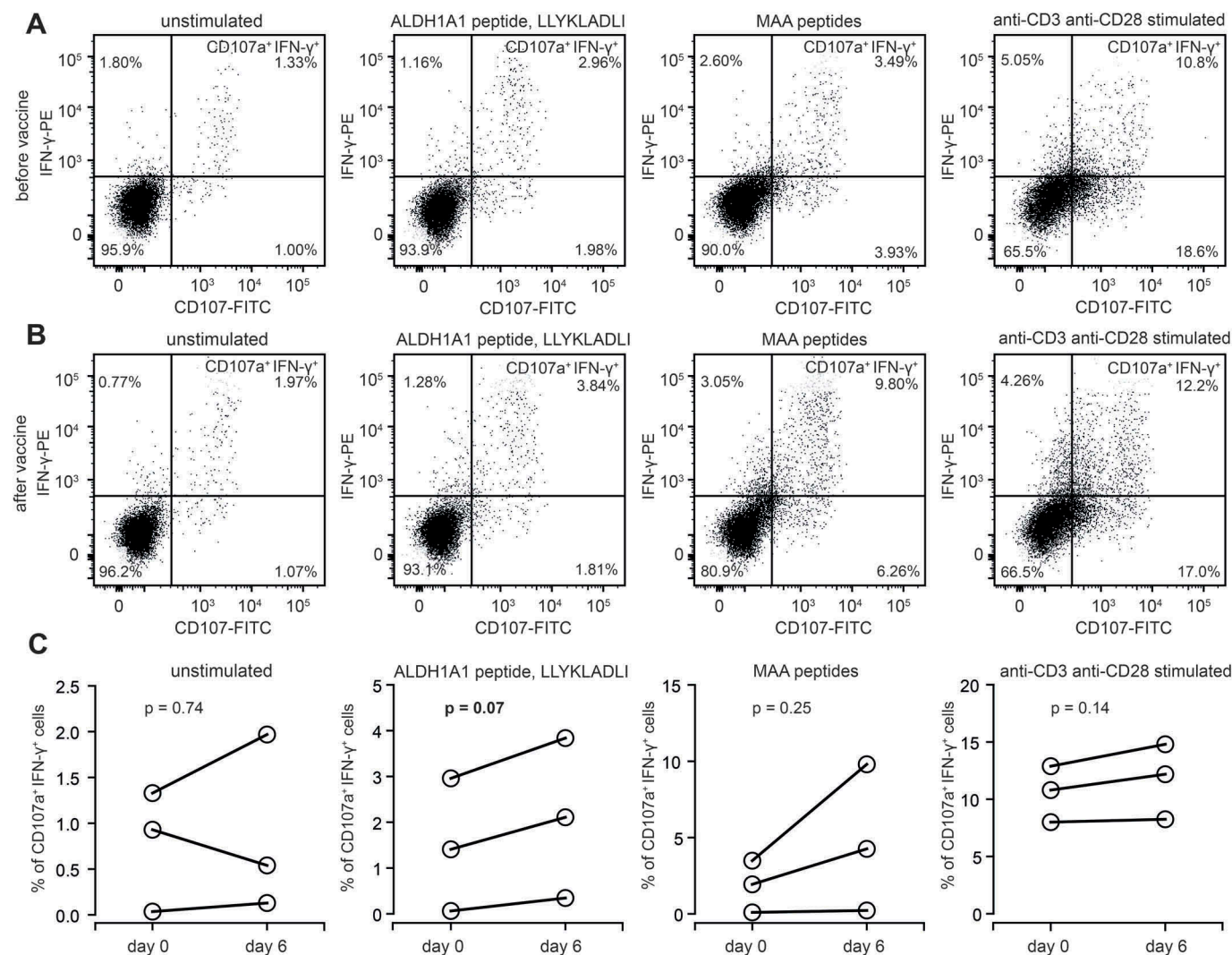


Figure 4. Functional activation of ALDH1-specific CD8⁺ cells in AGI-101H-treated melanoma patients upon vaccine administration. A. Representative dot plots presenting unstimulated, ALDH1A1 peptide stimulated, MAA peptides stimulated, and anti-CD3/anti-CD28 stimulated CD8⁺ T cells (from AGI-101H treated melanoma patient on the day of vaccine administration) stained with anti-CD107a and anti-IFN- γ . B. Representative dot plots presenting unstimulated, ALDH1A1 peptide stimulated, MAA peptides stimulated, and anti-CD3/anti-CD28 stimulated CD8⁺ T cells (from AGI-101H treated melanoma patient 6 days after vaccine administration) stained with anti-CD107a and anti-IFN- γ . C. Percentage of CD107a⁺IFN- γ ⁺ cells in unstimulated, ALDH1A1 peptide stimulated, MAA peptides stimulated, and anti-CD3/anti-CD28 stimulated CD8⁺ T cells (from AGI-101H treated melanoma patient on the day of vaccine administration and 6 days later).

Discussion

There are four major findings of the study, (i) the H6 modification of AGI-101H cells changed their phenotype towards MSC-like with the high activity of ALDH1A1; (ii) immunization of advanced melanoma patients with AGI-101H generated ALDH1A1-specific and functionally active CD8⁺ T cells; (iii) ALDH1A1-specific CD8⁺ T cells acquired central memory phenotype in AGI-101H treated patients; (iv) ALDH1-specific CD8⁺ T cells were found in untreated stage IV melanoma patients but not in stage II-III and healthy individuals.

STAT3 regulates cell proliferation, differentiation, and survival.¹⁰ Activation of STAT3 by phosphorylation has been reported in 70% of human cancers, including melanoma.¹¹ Moreover, it plays an important role in oncogenesis, and in the modeling of CSCs of various origins, including breast, lung, pancreas, and head and neck cancers.¹² JAK/STAT3 pathway may be activated via the IL-6 receptor complex comprising IL-6 – binding subunit

(gp80, IL-6R) and signal transducing subunit – gp130. IL-6 does not bind to gp130 making the IL-6R mandatory for gp130 activation. There are three activation mechanisms of the IL-6/gp130/JAK/STAT pathway, classical, transsignaling and cluster signaling.^{13,14} Classical involves membrane-bound gp80, which attracts gp130 subunits and transduces the signal, while transsignaling utilizes sIL-6R/gp130 complex. IL-6 transsignaling regulates mostly pro-inflammatory reactions.¹⁵ Since gp80 is expressed on a limited number of cells such as hepatocytes, some epithelial or some leukocytes, the transsignaling pathway is more general, thus other cells, which do not possess IL-6R are targeted. Hyper-IL-6 (H6) is a fusion protein comprising sIL-6R and gp130 bound by artificial linker and directly targets gp130.⁶ The biological activity of H6 is much broader and many times higher than sIL-6R/gp130 soluble complex. H6 cDNA was stably transduced into Mich1 and Mich2 cells using double copy bicistronic retroviral vector.⁵ H6 secreted by the cells

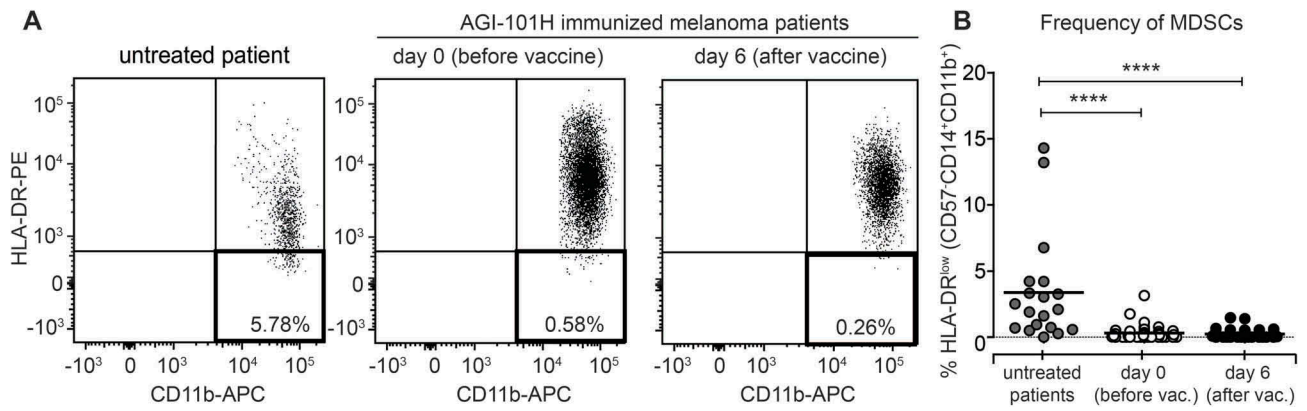


Figure 5. AGI-101H treatment decreased the number of circulating Myeloid-Derived Suppressor Cells (MDSCs) in treated patients. A. Flow cytometry analysis of MDSC cells characterized by the CD57-CD11b+CD14+HLA-DR- phenotype. Representative plots from AGI-101H vaccinated melanoma patient at day 0 and day 6 after vaccination are depicted. B. Cytometric data of multiparametric analysis of the frequency of MDSC cells obtained for healthy controls ($n = 14$), untreated patients ($n = 20$), and AGI-101H-vaccinated patients ($n = 57$) at day 0 and at day 6, were statistically analyzed using Kruskal-Wallis test, $p < 0.0001$. Differences between groups were tested using the Mann Whitney U test. Data are presented as dot plots with mean shown as a line.

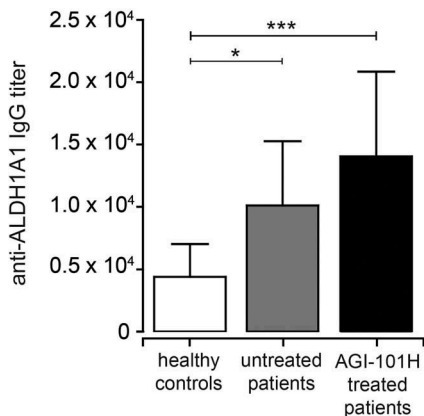


Figure 6. Immunization with AGI-101H enhances humoral response to ALDH1 antigen. The graph shows the titers of anti-ALDH1 IgG determined as the reciprocal of the highest serum dilution giving OD value at least two-fold higher than the background. Data obtained with ELISA were statistically analyzed using the Kruskal-Wallis test, $p < 0.0001$. Differences between groups were tested using Mann Whitney U test: **** $p < 0.0001$, ** $p = 0.0027$, * $p = 0.037$. Data are presented as mean with SD.

of both vaccine lines led to their autostimulation, what resulted in STAT3 tyrosinases phosphorylation and alteration of the phenotype of the cell towards MSC-like. Moreover, activation of gp130 also affects MAP and PIK3 pathways.

Efficient induction of specific immune response requires proper priming. Irradiated, life AGI-101H cells with H6 as molecular adjuvant provided complex priming comprising of delivery of MSC and differentiated melanoma antigens, allogeneic stimulation, apoptotic bodies or cytokines such as IL-12 and IFN- γ . H6 at the site of vaccine administration enhanced activation of CD8⁺ T cells¹⁶ including allogeneic CD8⁺ T cell response (not published), induced production of GM-CSF,¹⁷ presentation of cryptic antigens and maturation of DCs, inhibition of regulatory T cells formation by inhibition of FoxP3 expression,¹⁸ stimulation of B cells to antibody production. Downstream in the circulation CTL specific for melanoma antigens including ALDH1A1₈₈₋₉₆, NY-ESO, gp-100 and Tyrosinase were found, NK cells significantly

activated, while the number of monocytic myeloid-derived suppressor cells was reduced (data not published).

Visus et al.¹⁹ have demonstrated that AHDL1A1₈₈₋₉₆ peptide is naturally presented, HLA-A2 restricted and CD8⁺ T cell defined antigen expressed in squamous cell carcinoma of the head and neck. Using tumor-specific CD8⁺ T cells, they identified ALDH1A1 as a novel tumor antigen. Subsequently, Visus et al.²⁰ showed that ALDH^{bright} tumor cells in human cancers were recognized by HLA-A2 restricted AHDL1A1₈₈₋₉₆ peptide specific CD8⁺ T cells and eliminated *in vitro* and *in vivo*. Moreover, in human tumor xenograft models they have demonstrated that adoptive transfer of ALDH1A1 specific CD8⁺ T cells inhibited the growth of subcutaneously implanted cells and induced lung metastases. Moreover, above therapy following surgical resection of primary tumor inhibited recurrence of the disease and extended survival of mice. Luo et al.²¹ have shown that ALDH1A isoenzymes are markers of human MSC as well. Moreover, they demonstrated that ALDH1-positive melanoma cells are more tumorigenic and more resistant to chemotherapeutics in mice models. AHDL1A1 silencing led to cell cycle arrest, apoptosis, decreased cell viability *in vitro* and reduced tumorigenesis *in vivo*.²² Abovementioned findings indicated that ALDH1 isoenzymes are also possible therapeutic targets for melanoma. At the same time, Lu et al.²³ reported targeting murine MSC via dendritic-cell (DC) vaccination using DCs pulsed with ALDH^{bright} cell lysates, which significantly inhibited tumor growth as compared with DCs pulsed with either ALDH^{dim} or whole tumor lysates. Moreover, in serum from these mice IgG antibodies that bound ALDH^{bright} cells and mediated their complement-dependent lysis were found. In addition, PBMC and splenocytes from ALDH^{bright} lysate-pulsed DCs were more cytotoxic than ALDH^{dim} DCs. Finally, HLA-A2-restricted, AHDL1A1₈₈₋₉₆-specific CD8⁺ T cells were detected in the circulation of head and neck squamous cell carcinoma patients.¹⁹ In addition, Taylor et al. demonstrated that high ALDH1 expression correlated with better prognosis in melanoma.²⁴ Interestingly, normal stem cells for example hematopoietic stem cells also express ALDH1A1, but at the lower level than tumor cells. It was also shown that they are

not recognized by ALDH1A1-specific CD8⁺ T cells. Thus immuno-targeting of melanoma ALDH1A1 positive cells should not be toxic.¹⁹ In our clinical trials, we have applied 30 000 vaccine doses so far, and we did not see any systemic adverse events related to the treatment.

Here we report for the first time generation of ALDH1A1-specific CD8⁺ T cells and anti-ALDH1A1 antibodies in patients immunized with whole cell melanoma vaccine genetically modified to displaying MSC-like phenotype. In all HLA-A2 positive long living patients, ALDH1A1-specific CD8⁺ T cells were detected. Since ETAM trial is a continuation of treatment study,^{8,9} we could not evaluate the baseline level of these specific CD8⁺ T cells before immunization. Accordingly, we have investigated ALDH1A1-specific CD8⁺ T cells before and following vaccine dose administrations in long-living treated patients. We found that the number of ALDH1A1-specific CD8⁺ T cells significantly increased after 6 days post vaccination and until the next dose administration returned to the previous level. Accordingly, to maintain the long-lasting anti-melanoma immune response the continuous vaccine boosting was required.^{25,26} We failed to demonstrate ALDH1A1-specific CD8⁺ T cells in the circulation of healthy donors. However, in a fraction of advanced melanoma untreated patients, mostly with stage IV and measurable metastases, but not with stage II-IIIC we found ALDH1A1-specific CD8⁺ T cells, but the number of cells was significantly lower than in vaccine treated patients. Circulating ALDH1A1-specific CD8⁺ T cells acquired central memory phenotype and were functionally active. Analyzes of untouched blood-derived CD8⁺ T cells from treated patients demonstrated non-specific degranulation and IFN- γ secretion before dose administration, which further increased after 6 days. Analyzes of specific CD8⁺ T cells following peptide (AHD1A1₈₈₋₉₆) 6 hours of stimulation *ex vivo* had shown specific degranulation and IFN- γ secretion before next dose immunization, which also increased after 6 days after that. Schaefer et al.²⁷ have shown the correlation between melanoma peptide-specific CD8⁺ T cells functionality but not phenotype with survival in the multi-epitope peptide vaccine trial. Beyond ALDH1A1 we have also found and used as comparator induction of specific, functional CD8⁺ T cells for three “classical” melanoma associated antigens: NY-ESO, gp100, and tyrosinase in the circulation of treated patients which were also used as comparators in the degranulation experiments.

Moreover, we have also observed that AGI-101H treatment decreased the number of circulating Myeloid-Derived Suppressor Cells (MDSCs) in treated patients. MDSCs are a heterogeneous population of immature bone marrow-derived myeloid cells, including myeloid progenitors and precursors of macrophages, granulocytes and dendritic cells.²⁸ They have been identified in cancer patients and in experimental animals as cells with the ability to suppress activation and proliferation of T lymphocytes. It has been demonstrated in a number of studies that MDSCs are correlated with the development of malignancies.

Infiltration of MDSCs has been observed in solid tumors and increased numbers of MDSCs were associated with cancer progression, immune dysfunction, and poor prognosis.²⁹⁻³⁴ In patients with non-small cell lung cancer, both frequency and

the absolute number of peripheral CD14⁺HLA-DR^{-low} MDSCs subset were significantly increased compared with healthy controls and were associated with metastasis, response to chemotherapy and progression-free survival.³⁵ In patients with terminal cancer, peripheral blood levels of granulocytic MDSCs correlated with overall survival. Patients with low levels of CD15⁺CD16^{low} cells had significantly longer survival times and patients with high levels of CD15⁺CD16^{low} cells tended to have poor performance status.³⁶ High frequencies of CD57⁺HLA-DR⁻CD11b⁺CD33⁺ cells were associated with decreased overall survival in gastrointestinal malignancies, pancreatic cancer, and breast cancer.³⁶⁻³⁹

In melanoma patients with advanced disease various monocytic (CD14⁺HLA-DR^{-low}, CD14⁺IL4Ra⁺) and granulocytic (CD57⁺HLA-DR⁻CD33⁺CD15⁺IL-4Ra⁺, CD14⁻CD66b⁺Arginase1⁺) MDSCs populations are elevated.⁴⁰⁻⁴³ It was reported that enrichment in MDSC population was associated with elevated amounts of inflammatory factors such as IFN- γ , IL-1 β , and CXCL10 that support MDSC activation and accumulation.⁴⁴ Recently Rudolph et al. observed accumulation of CD11b⁺CD33⁺CD14⁺HLA-DR^{-low} MDSCs in all stages of melanoma, including early stage I patients.⁴⁵ Moreover, circulating monocytic MDSCs were reported to have the negative impact on survival in patients with advanced melanoma and have independent prognostic value.^{46,47} Furthermore, MDSCs inversely correlated with the presence of functional antigen-specific T cells and patients with high MDSCs levels had more PD-L1 T cells and more CTLA-4 expression by regulatory T cells.⁴⁷ In patients with non-small cell lung cancer, circulating MDSCs negatively correlated with immune response to cancer vaccine and targeting MDSC substantially improved immune response to vaccination.^{48,49}

The action of AGI-101H on the immune system of treated melanoma patient leads on one side to the activation of tumor-specific lymphocytes, including T cell specific for antigens of cancer initiating cells. On the other side, there is an evidence, that the vaccine, either directly or through secreted mediators such as H6, influence the population of MDSCs in treated patients, by leading to its reduction. However, the exact mechanisms behind this phenomenon are to be discovered.

Finally, AGI-101H immunization generated specific antibodies towards ALDH1 protein in treated patients. As mentioned above these antibodies analyzed in animal models were able to eliminate ALDH1 positive melanoma stem cells by antibody dependent cell cytotoxicity.²³

Discovery of the role played by the immune checkpoints and tumor microenvironment in the anti-cancer immune responses has changed the philosophy of immunotherapeutic approaches. Therapeutic vaccination successfully induces specific responses, however, formed tumors using immune-checkpoint synapses block tumor eradication. Accordingly, the patients with resected metastases are the best targets for therapeutic vaccination in the adjuvant setting. However, in a fraction of patients, tumors may return, what results in turning off the immune defense mechanisms and progression. In our study protocol in case of progression, we applied more frequent dosing, what resulted in many cases metastatic tumor eradication.⁹ In the fraction of cases, we excised

returning tumors first and continued immunization until patients' death. Above strategy resulted in long-term survival of a significant number of advanced melanoma patients.⁹ On the other hand blockade of immune checkpoints prevents elimination of specific CTL entering the tumor. However, these CTL may become exhausted and lose the effectiveness. Accordingly, more specific functional CTL are required. They might be provided by cancer vaccination, especially those, which immune-target CSC.

Materials and methods

Patients

Long-term survivors enrolled into ETAM2-5 Trial (Extended Treatment of Advanced Melanoma Patients Transferred from Trials 2-5; EudraCT Number 2008-003373-40) were studied.^{8,9} ETAM was initiated in November 2008, and all 138 surviving patients from trials 2-5 were transferred. The Regional Bioethics Committee approved the clinical study; all patients signed the informed consent. As of October 25, 2017, 106 patients including 39 HLA-A2 positive were alive. HLA-A2 positive patients form the study group and continue the treatment (Table 1). The majority of HLA-A2 patients (n = 35) before transferring into ETAM participated in two adjuvant studies (TRIAL 3 and TRIAL 5) evaluating AGI-101H vaccine in patients with resected metastases.⁹ The remaining 4 patients participated in two other studies (TRIAL 2 and 4) evaluating AGI-101H in non-resectable metastatic melanoma.⁸ The mean time of treatment was 154 months ranging from 128 to 202. At the time of blood sampling, all patients treated with AGI-101H were free of clinically manifested melanoma. Blood was collected before subsequent vaccine administration and 6 days after that.

The control group included 24 HLA-A2 positive advanced melanoma patients who were not treated and gave written informed consent. Seven patients had resected metastatic melanoma, while 17 had the non-resectable metastatic disease. In patients with resected melanoma sampling was performed following surgical resection of the metastases into regional lymph nodes. In patients with the non-resectable disease, sampling was carried out prior to the initiation of AGI-101H therapy. Ten healthy HLA-A2 positive donors, who gave written informed consent were also included in the study.

A vaccine composition, dosing, and combination with surgery

AGI-101H is allogeneic whole cell gene modified therapeutic vaccine composed of two allogeneic human melanoma cell lines, Mich1H6 and Mich2H6, manufactured according to GMP requirements. Mich1H6 and Mich2H6 cells were stably transduced with designer molecular adjuvant Hyper-IL-6 (H6) cDNA using double copy bicistronic retroviral vector.^{5,6} Mich1H6 and Mich2H6 cells were admixed 1:1, irradiated with 80Gy and stored in liquid nitrogen. AGI-101H was administered to patients in adjuvant setting 8 times in two-week intervals (induction phase) and then once a month until death (maintenance phase). In case of recurrence, the induction phase was repeated with or without surgery and followed by maintenance.⁹ In patients with measurable metastases, the induction phase was applied. At progression, further management was at the discretion of the clinician. Usually, re-induction followed by maintenance was used. If clinically indicated, palliative radiotherapy during vaccine treatment was permitted. Maintenance was not interrupted in case of disease progression.⁸

Cell culture conditions for in vitro experiments

Mich1, Mich2, Mich1H6 and Mich2H6 cells were cultured in DMEM High Glucose medium (Biowest Europe cat. no. L0102) supplemented with 10% foetal bovine serum (Biowest Europe cat. no. S181H) and Penicillin-Streptomycin (Sigma-Aldrich cat. no. P4333) in a humidified atmosphere containing 5% CO₂/95% air at 37°C.

ALDEFLUOR assay

Intracellular ALDH enzymatic activity was measured using the ALDEFLUOR kit (STEMCELL Technologies Inc cat. no. D1700). Cultured Mich1, Mich2, Mich1H6 and Mich2H6 cells were resuspended to a concentration of 2×10^5 cells/mL with the ALDEFLUOR Assay Buffer and incubated with the activated ALDEFLUOR Reagent for 45 minutes at 37°C according to the manufacturer's instructions. For a negative control ALDEFLUOR DEAB Reagent, the specific ALDH inhibitor diethylaminobenzaldehyde, was added to all samples before

Table 1. Patients characteristics.

Characteristics	AGI-101H vaccine group	Control group
Patients	39	24
Age (median)	61	57
Male	15	12
Female	24	12
Stage		
II	-	1
IIIA	-	2
IIIB	18	4
IIIC	13	-
IV	8	17
Disease status	Resected melanoma: 35 patients Unresectable: 4 patients	Resected melanoma: 7 patients Unresectable: 17 patients
Treatment	AGI-101H adjuvant setting: 35 patients AGI-101H palliative setting: 4 patients	None None
Time of treatment (mean)	adjuvant setting: 153 months (128–202) palliative setting: 156 months (131–179)	N/A

incubation. Samples were analyzed with FACSAria flow cytometer (BD Biosciences) and FlowJo software (Tree Star Inc.).

Vaccine immunophenotyping

For the assessment of CD44 and PD-L1 expression, APC-mouse anti-human CD44 (Pharmingen cat. no. 559942) or PE-mouse anti-human 274 (PD-L1 Biologend cat. no. 329706) were used. For analyzes of PD-1, PE-Cy7- mouse anti-human CD279 (PD-1, Biologend cat. no. 329198) was applied in flow cytometry. For Signal Transducer and Activator of Transcription 3 (STAT3) phosphorylation, 1×10^6 cells were incubated with Fixation Buffer (BD Biosciences cat. no. 554655), washed with PBS (Biowest Europe cat. no. L0615) (1mM sodium orthovanadate, Sigma cat. no. 56508), and permeabilized with ice-cold 100% methanol (Sigma cat. no. 900641-4X). Cells were then stored in -80°C until intracellular staining with Alexa Fluor[®] 647 Mouse Anti-Stat3 (pS727, BD Biosciences cat. no. 558099) or Alexa Fluor[®] 647 Mouse Anti-Stat3 (pY705, BD Biosciences cat. no. 557815) and analysis on FACSCanto.

Protein extraction and immunoblot analysis

Cells were washed twice with phosphate buffered saline (PBS; Biowest Europe cat. no. L0615) and collected into fresh tubes using cell scrapers. Proteins were extracted in ice-cold 1x RIPA lysis buffer (Sigma-Aldrich cat. no. R0278) containing 10x diluted protease inhibitor cocktail (Sigma-Aldrich cat. no. P8340). Extracts were kept on ice for 20 min and centrifuged at 13,000 RPM for 15 min at 4°C . Supernatants were stored at -80°C . Proteins were quantified by BCA assay (Thermo Fisher Scientific cat. no. 23227). For immunoblotting 30 μg of whole protein extracts were loaded onto 4–20% gradient polyacrylamide gels (Bio-Rad Laboratories) and separated by SDS-PAGE. Proteins were then electro-blotted onto PVDF membranes (Bio-Rad Laboratories) using a Trans-Blot Turbo Transfer System (Bio-Rad Laboratories cat.no. 170-4156). Unspecific binding sites were blocked using 5% BSA (Sigma-Aldrich cat. no. A1470) resolved in Tris-buffered saline containing 0.1% Tween 20 (Sigma-Aldrich cat. no. P94-16) (TBS-T) (further referred to as blocking buffer). Primary monoclonal antibodies: anti-human MITF or anti-human ABCB5 (Thermo Fisher Scientific) were diluted 1:500 in blocking buffer and incubated overnight at 4°C with the respective fragments of the membrane. After washing the membranes were incubated with anti-mouse IgG antibody conjugated to horseradish peroxidase (HRP; Cell Signaling Technology, Danvers, MA), diluted 1:1000 in blocking buffer. All washing steps were performed using TBS-T buffer. Proteins were visualized by chemiluminescence using WesternBright Quantum HRP substrate (Advansta, Menlo Park, CA cat. no. K-12042-D20) and CCD imager G:BOX (Syngene, Cambridge, UK).

Peripheral blood mononuclear cells (PBMC) isolation

Peripheral blood was obtained from melanoma patients treated with AGI-101H, untreated melanoma patients and healthy donors under sterile conditions in heparinized tubes (BD

Biosciences cat. no. REF368480). PBMCs were isolated within 3 hours of blood collection by standard gradient centrifugation in Histopaque 1077 (Sigma-Aldrich cat. no. 10771) and were used for dextramer staining. The remaining cells were cryopreserved using CTL-Cryo™ ABC Media Kit (C.T.L. cat. no. GTLC-ABC), that ensures unimpaired PBMC functions, and used for T cell functional analyses. After thawing, cells were directly used in ELISPOT or CD117a/IFN- γ assays.

HLA typing

PBMCs were tested for expression of HLA-A2 antigens by flow cytometry using PE-labeled BB7.2 monoclonal antibody (BioLegend cat. no. 343306). Samples were analyzed on a FACSCanto (BD Biosciences) using BD FASCDiva v.6.1.2 software.

Dextramer staining

Freshly isolated PBMCs (2 million) were washed once with PBS containing 5% FBS and re-suspended in a total volume of 50 μl PBS with 5% FBS. Cells were incubated with PE-labeled HLA-A0201 MHC dextramers loaded with AHD1A1₈₈₋₉₆ (LLYKLADLI) or negative control peptides (Immudex cat. no. WB3794, cat. no. WB2666) in the dark at room temp. for 10 min, according to the manufacturer's instructions. Next, cells were labeled with recommended amounts of anti-CD3-PE-Cy7 (clone SK-7, BioLegend cat. no. 344816), anti-CD8-APC (clone RPA-T8, BioLegend cat. no. 301049) and anti-CD4-FITC (clone SK3, BD Biosciences cat. no. 347413) monoclonal antibodies in the dark at 4°C for another 20 min. Labeled cells were washed twice with PBS with 5% FBS, and dead cells were stained with 7-AAD (BD Biosciences cat. no. 559925) in the dark for 10 min. Cells were resuspended in 0.4 ml PBS and immediately analyzed on a FACSCanto flow cytometer. Data acquisition was performed using BD FASCDiva v.6.1.2. Dextramer positive cells were analyzed within CD3⁺CD8⁺ gate, after the exclusion of doublets, CD4⁺, and dead cells. Supplemental [Figure 1](#) presents the gating scheme for the analysis of ALDH1A1₈₈₋₉₆-specific CD8⁺ T cells.

Dextramer-positive cell phenotyping

Frozen PBMCs from HLA-A2 patients (at least 30×10^6 cells at day 0 and 6 days after vaccination) were thawed as previously described.⁵⁰ Cells were washed twice with ice-cold PBS and were further subjected to magnetic bead separation with human CD8⁺ T Cell Isolation Kit (Miltenyi Biotec cat. no. 130-096-495). The purity of separation was determined with FACS analysis of CD3 (anti-CD3-PE-Cy7; clone SK-7, BioLegend cat. no. 344816) and CD8 (anti-CD8a-FITC; clone RPA-T8, BioLegend cat.no. 301006) cell surface markers. Separated cells were resuspended in a total volume of 50 μl PBS. Cells were incubated with PE-labeled HLA-A0201 MHC dextramers loaded with AHD1A1₈₈₋₉₆ (LLYKLADLI) or negative control peptides (Immudex cat.no. WB3794, cat. no. WB2666) in the dark at room temperature for 10 min, according to manufacturer's instructions. Next, cells were labeled with

recommended amounts of anti-CD3-PE-Cy7 (clone SK-7, BioLegend cat. no. 344816), anti-CD8a-FITC (clone RPA-T8, BioLegend cat. no. 301006), anti-CD45-APC (clone HI100, BD Biosciences cat. no. 304112), and anti-CCR7-PerCP/Cy5.5 (clone G043H7, BioLegend cat. no. 353220) monoclonal antibodies in the dark at 4°C for another 20 min. Labeled cells were washed twice with PBS, resuspended in 0.4 ml PBS, and immediately analyzed on a FACSCanto flow cytometer. Data acquisition was performed using BD FACSDiva v.6.1.2.

Degranulation of CD8⁺ T cells in vitro

1×10^6 PBMC was suspended in X-Vivo 15 medium (Lonza, Verviers cat. no. BE04-744Q), incubated with or without AHDL1A1₈₈₋₉₆ (LLYKLADLI) antigenic peptide (Immudex cat. no. WB3794) at 0.2 µg/ml. As a reference, PBMCs were stimulated with mixed Melanoma Associated Antigens: NY-ESO, gp-100 and Tyrosinase peptides (Think Peptides, ProMix Pre-mixed Peptide Libraries cat. codes: PX-NYESO, PX-GP100, PX-TYR) at 0.1 µg/ml or purified NA/LE mouse anti-human CD3 (BD Biosciences cat. no. 555336) plus anti-human CD28 antibodies (BD Biosciences cat. no. 555725) at 1 µg/ml. PBMCs were stimulated in cytometric tubes at 37°C in a humidified 5% CO₂ atmosphere for 6 hours, in the presence of FITC-conjugated mouse anti-human CD107a antibody (clone H4A3, BD Biosciences cat. no. 555800). After one-hour monensin (Sigma Aldrich cat. no. M5273, 50 µg/ml) and BrefeldinA (BD Biosciences cat. no. 555029, 50 µg/ml) were added. Next, cells were washed, and surface stained with PE-Cy7-conjugated mouse anti-human CD3 (clone SK7, Biolegend cat. no. 344816) and APC-conjugated mouse anti-human CD8 (clone RPA-T8 Biolegend cat. no. 301049) antibodies at 4°C for 30 min. Then cells were washed with Stain Buffer (BD Pharmigen cat. no. 554656) and fixed using BD Cytotfix/Cytoperm™ Fixation/Permeabilization Solution (BD Pharmigen cat. no. 51-2090KZ) at room temp. for 20 min. Fixed cells were washed with BD Perm/Wash buffer (cat. no. 51-2091KZ) stained with PE-conjugated anti-IFN-γ (clone B27, BD Biosciences cat. no. 554701) at room temp. for 30 min, washed again with BD Perm/Wash buffer and analyzed using FACSCanto flow cytometer. A minimum of 1×10^5 CD3⁺CD8⁺ events was required for analyses.

Detection of myeloid-derived suppressor cells (MDSCs) in patients

Frozen PBMCs from HLA-A2 patients (at least 30×10^6 cells at day 0 and 6 days after vaccination) were thawed as previously described.⁵⁰ Cells were washed twice with ice-cold PBS and were incubated with Human TrueStainFcXTM Fc Receptor Blocking Solution (BioLegend cat. no. 422301) at room temp. for 5 min to block non-specific binding of antibodies. Next, cells were labeled with recommended amounts of anti-CD3-FITC (BD Biosciences cat. no. 555916), anti-CD19-FITC (BD Bioscience cat. no. 555412), anti-CD20-FITC (BD Bioscience cat. no. 555622), anti-CD57-FITC (BD Bioscience cat. no. 555619), anti-CD56-FITC (BD Bioscience cat. no. 562794), anti-HLA-DR-PE

(BD Bioscience cat. no. 555812), anti-CD14-PerCP-Cy5.5 (BioLegend cat. no. 301823) and anti-CD11b-APC (BioLegend cat. no. 301310) at 4°C in the dark for 30 min. Labeled cells were washed twice with PBS, resuspended in 0.4 ml PBS, and immediately analyzed on a FACSCanto flow cytometer. Data acquisition was performed using BD FACSDiva v.6.1.2.

Serum preparation and anti-ALDH1 antibody ELISA

Serum samples were collected after 2 hours of the whole blood sample clotting and were stored at -20°C. The titer of anti-ALDH1 antibodies was measured by ELISA. The MaxiSorp 96-well plates (Nunc™ ThermoFisher Scientific) were coated with the purified recombinant human ALDH1 protein (Immunogen cat. no. WB3794) at a concentration of 1 µg/ml in PBS. 100 µl of the antigen solution was added to each well and incubated overnight at 4°C. Plates were washed with PBS/0.1% Tween 20 (PBS-T) and 1% BSA in PBS for 2 hours at room temp. and incubated overnight at 4°C. For each serum sample, eight serial dilutions (in PBS) were prepared, starting from 500× and run in duplicates. PBS was used as a blank. After overnight incubation, the plates were washed with PBS-T and incubated with 100 µl of HRP-conjugated anti-human IgG detection antibody (Abcam) at room temp. for 1 hour. Next, the plates were incubated with substrate solution (OPD, Sigma-Aldrich cat. no. P9187) for 20 min at room temp. and read by a spectrophotometer at 450 nm. The titer was determined as the reciprocal of serum dilution where the optical density (OD) value was at least two-fold higher than the OD value of the blank sample.

Statistical analyses

Numerical data were expressed as a mean and standard deviation. Analyses of paired data were performed using the Wilcoxon matched-pairs signed rank test. Differences in means were evaluated with the non-parametric Mann-Whitney U test based on distribution levels. Multiple groups were compared with the Kruskal-Wallis test. The statistical analysis was performed with GraphPad Prism Version 6.0 software. The level of statistical significance was defined as $p < 0.05$.

Disclosure of interest

The authors report no conflict of interest.

Funding

This work was supported by the National Center for Research and Development (Warsaw, Poland) under Grant: INNOMED/6/I/NCBR/2014, "Personalization of melanoma therapeutic vaccination (Per-Mel)".

ORCID

Eliza Kwiatkowska-Borowczyk  <http://orcid.org/0000-0003-1620-7965>
 Patrycja Czerwińska  <http://orcid.org/0000-0003-2400-1174>
 Katarzyna Tomela  <http://orcid.org/0000-0002-3622-7229>

Anna Karolina Kozłowska  <http://orcid.org/0000-0003-2465-217X>
 Ewelina Dondajewska  <http://orcid.org/0000-0001-9078-2015>
 Monika Żakowska  <http://orcid.org/0000-0003-4657-4352>
 Andrzej Mackiewicz  <http://orcid.org/0000-0001-8570-0863>

References

- Mackiewicz J, Mackiewicz A. Programmed cell death 1 checkpoint inhibitors in the treatment of patients with advanced melanoma. *Contemp Oncol (Pozn)*. 2017;21(1):1–5. doi:10.5114/wo.2017.66651.
- Noman MZ, Hasmim M, Messai Y, Terry S, Kieda C, Janji B, Chouaib S. Hypoxia: a key player in antitumor immune response. A review in the theme: cellular responses to hypoxia. *Am J Physiol Cell Physiol*. 2015;309(9):C569–79. doi:10.1152/ajpcell.00207.
- Reya T, Morrison SJ, Clarke MF, Weissman IL. Stem cells, cancer, and cancer stem cells. *Nature*. 2001;414:105–111. doi:10.1038/35102167.
- Kwiatkowska-Borowczyk EP, Gąbka-Buszek A, Jankowski J, Mackiewicz A. Immunotargeting of cancer stem cells. *Contemp Oncol (Pozn)*. 2015;19(1A):A52–9. doi:10.5114/wo.2014.47129.
- Wiznerowicz M, Fong AC, Mackiewicz A, Hawley RC. Development of dicistronic double copy retroviral vectors for human gene therapy. *Gene Ther*. 1997;4:1061–1068. doi:10.1007/978-1-4615-5357-1_68.
- Fisher M, Goldschmitt J, Peschel C, Brakenhoff JP, Kallen KJ, Wollmer A, Grotzinger J, Rose-John S. A bioactive designer cytokine for human hematopoietic progenitor cell expansion. *Nat Biotechnol*. 1997;15:142–145. doi:10.1038/nbt0297-142.
- Kozłowska A, Mackiewicz J, Mackiewicz A. Therapeutic gene modified cell based cancer vaccines. *Gene*. 2013;525(2):200–207. doi:10.1016/j.gene.2013.03.056.
- Mackiewicz J, Karczewska-Dzionk A, Laciak M, Kapcinska M, Wiznerowicz M, Burzykowski T, Zakowska M, Rose-John S, Mackiewicz A. Whole cell therapeutic vaccine modified with Hyper-IL6 for combinational treatment of nonresected advanced melanoma. *Medicine (Baltimore)*. 2015;94(21):e853. doi:10.1097/MD.0000000000000853.
- Mackiewicz A, Mackiewicz J, Wysocki PJ, Wiznerowicz M, Kapcinska M, Laciak M, Rose-John S, Izycki D, Burzykowski T, Karczewska-Dzionk A. Long-term survival of high-risk melanoma patients immunized with a Hyper-IL-6-modified allogeneic whole-cell vaccine after complete resection. *Expert Opin Investig Drugs*. 2012;21(6):773–783. doi:10.1517/13543784.2012.684753.
- Islam M, Sharma S, Teknos TN. RhoC regulates cancer stem cells in head and neck squamous cell carcinoma by overexpressing IL-6 and phosphorylation of STAT3. *PLoS One*. 2014;9:e88527. doi:10.1371/journal.pone.0088527.
- Yuan J, Zhang F, Niu R. Multiple regulation pathways and pivotal biological functions of STAT3 in cancer. *Sci Rep*. 2015;5:176. doi:10.1038/srep17663.
- Teng Y, Ross JL, Cowell JK. The involvement of JAK-STAT3 in cell motility, invasion, and metastasis. *JAKSTAT*. 2014;3(1):e28086. doi:10.4161/jkst.28086.
- Drucker C, Gewiese J, Malchow S, Scheller J, Rose-John S. Impact of interleukin-6 classic- and trans-signaling on liver damage and regeneration. *J Autoimmun*. 2010;34(1):29–37. doi:10.1016/j.jaut.2009.08.003.
- Mackiewicz A, Schooling H, Heinrich PC, Rose-John S. Complex of soluble human IL-6-receptor/IL-6 up-regulates expression of acute phase proteins. *J Immunol*. 1992;149:2021–2027.
- Rose-John S. IL-6 trans-signaling via the soluble IL-6 receptor: importance for the pro-inflammatory activities of IL-6. *Int J Biol Sci*. 2012;8:1237–1247. doi:10.7150/ijbs.4989.
- Bottcher JP, Schranz O, Garbes C, Zaremba A, Hegenbarth S, Kurts C, Beyer M, Schultze JL, Kastenmüller W, Rose-John S, et al. IL-6 trans-signaling-dependent rapid development of cytotoxic T cell function. *Cell Rep*. 2014;8:1318–1327. doi:10.1016/j.celrep.2014.07.008.
- Ozbek S, Peters M, Breuhahn K, Mann A, Blessing M, Fischer M, Schirmacher P, Mackiewicz A, Rose-John S. The designer cytokine hyper-IL-6 mediates growth inhibition and GM-CSF-dependent rejection of B16 melanoma cells. *Oncogene*. 2001;20(8):972–979. doi:10.1038/sj.onc.1204180.
- Dominitzki S, Fantini MC, Neufert C, Nikolaev A, Galle PR, Scheller J, Monteleone G, Rose-John S, Neurath MF, Becker C. Cutting edge: trans-signaling via the soluble IL-6R abrogates the induction of FoxP3 in Naive CD4+CD25- T cells. *J Immunol*. 2007;179:2041–2045. doi:10.4049/jimmunol.179.4.2041.
- Visus C, Ito D, Amoscato A, Maciejewska-Franczak M, Abdelsalem A, Dhir R, Shin DM, Donenberg VS, Whiteside TL, DeLeo AB. Identification of human aldehyde dehydrogenase 1 family member A1 as a novel CD8+ T-cell derived tumor antigen in squamous cell carcinoma of the head and neck. *Cancer Res*. 2007;67:10538–10545. doi:10.1158/0008-5472.CAN-07-1346.
- Visus C, Wang Y, Lozano-Leon A, Ferris RL, Silver S, Szczepanski MJ, Brand RE, Ferrone CR, Whiteside TL, Ferrone S, et al. Targeting ALDHbright human carcinoma-initiating cells with ALDH1-specific CD8+ T cells. *Clin Cancer Res*. 2011;17:6174–84. doi:10.1158/1078-0432.CCR-11-1111.
- Luo Y, Dallaglio K, Chen Y, Robinson WA, Robinson SE, McCarter MD, Wang J, Gonzalez R, Thompson DC, Norris DA, et al. ALDH1A1 isozymes are markers of human melanoma stem cells and targets for therapy. *Stem Cells*. 2012;10:2100–2113. doi:10.1002/stem.1193.
- Yue L, Huang Z-M, Fong S, Leong S, Jakowatz JG, Charruyer-Reinwald A, Wei M, Ghadially R. Targeting ALDH1 to decrease tumorigenicity, growth, and metastases of human melanoma. *Melanoma Res*. 2015;25:138–148. doi:10.1097/CMR.0000000000000144.
- Lu L, Tao H, Chang AE, Hu Y, Shu G, Chen Q, Egenti M, Owen J, Moyer MEP, Huang S, et al. Cancer stem cell vaccine inhibits metastases of primary tumors and induces humoral immune responses against cancer stem cells. *Oncoimmunology*. 2015;4(3):e990767. doi:10.4161/2162402X.2014.990767.
- Taylor LA, Abraham RM, Tahirovic E, van Belle P, Li B, Huang L, Elder DE, Gimotty P, Xu X. High ALDH1 expression correlated with a better prognosis of malignant melanoma. *Mod Pathol*. 2017;30(5):634–639. doi:10.1038/modpathol.2016.226.
- Nawrocki S, Mackiewicz A. Clinical trials of active cancer immunotherapy. *Expert Opin Investig Drugs*. 2007;16:1137–1141. doi:10.1517/13543784.16.8.1137.
- Mackiewicz J, Mackiewicz A. Design of clinical trials for therapeutic cancer vaccines development. *Eur J Pharmacol*. 2009;625(1–3):84–89. doi:10.1016/j.ejphar.2009.09.069.
- Schaefer C, Butterfield LH, Lee S, Kim GG, Visus C, Albers A, Kirkwood JM, Whiteside TL. Function but not phenotype of melanoma peptide-specific CD8+ T cells correlate with survival in a multi-peptide vaccine trial (ECOG 1696). *Int J Cancer*. 2012;131:874–884. doi:10.1002/ijc.26481.
- Keskinov AA, Shurin MR. Myeloid regulatory cells in tumor spreading and metastasis. *Immunobiology*. 2015;220:236–242. doi:10.1016/j.imbio.2014.07.017.
- Gabrivovich DI, Nagaraj S. Myeloid-derived suppressor cells as regulators of the immune system. *Nat Rev Immunol*. 2009;9:162–174. doi:10.1038/nri2506.
- Marigo I, Dolcetti L, Serafini P, Zanovello P, Bronte V. Tumor-induced tolerance and immune suppression by myeloid derived suppressor cells. *Immunol Rev*. 2008;222:162–179. doi:10.1111/j.1600-065X.2008.00602.x.
- Kapanadze T, Gamrekashvili J, Ma C, Chan C, Zhao F, Hewitt S, Zender L, Kapoor V, Felsner DW, Manns MP, et al. Regulation of accumulation and function of myeloid-derived suppressor cells in different murine models of hepatocellular carcinoma. *J Hepatol*. 2013;59:1007–1013. doi:10.1016/j.jhep.2013.06.010.
- Mace TA, Ameen Z, Collins A, Wojcik S, Mair M, Young GS, Fuchs JR, Eubank TD, Frankel WL, Bekaii-Saab T, et al. Pancreatic cancer-associated stellate cells promote differentiation

- of myeloid-derived suppressor cells in a STAT3-dependent manner. *Cancer Res.* 2013;73:3007–3018. doi:10.1158/0008-5472.CAN-12-4601.
33. Filipazzi P, Huber V, Rivoltini L. Phenotype, function and clinical implications of myeloid-derived suppressor cells in cancer patients. *Cancer Immunol Immunother.* 2012;61:255–263. doi:10.1007/s00262-011-1161-9.
 34. Lu T, Ramakrishnan R, Altiok S, Youn JI, Cheng P, Celis E, Pisarev V, Sherman S, Sporn MB, Gabrilovich D. Tumor-infiltrating myeloid cells induce tumor cell resistance to cytotoxic T cells in mice. *J Clin Invest.* 2011;121:4015–4029. doi:10.1172/JCI45862.
 35. Huang A, Zhang B, Wang B, Zhang F, Fan KX, Guo YJ. Increased CD14(+)HLA-DR (-/low) myeloid-derived suppressor cells correlate with extrathoracic metastasis and poor response to chemotherapy in non-small cell lung cancer patients. *Cancer Immunol Immunother.* 2013;62:1439–1451. doi:10.1007/s00262-013-1450-6.
 36. Choi J, Suh B, Ahn YO, Kim TM, Lee JO, Lee SH, Heo DS. CD15+/CD16low human granulocytes from terminal cancer patients: granulocytic myeloid-derived suppressor cells that have a suppressive function. *Tumour Biol.* 2012;33:121–129. doi:10.1007/s13277-011-0254-6.
 37. Gabitass RF, Annels NE, Stocken DD, Pandha HA, Middleton GW. Elevated myeloid-derived suppressor cells in the pancreatic, esophageal and gastric cancer are an independent prognostic factor and are associated with significant elevation of the Th2 cytokine interleukin-13. *Cancer Immunol Immunother.* 2011;60:1419–1430. doi:10.1007/s00262-011-1028-0.
 38. Solito S, Falisi E, Diaz-Montero CM, Doni A, Pinton L, Rosato A, Francescato S, Basso G, Zanovello P, Onicescu G, et al. A human promyelocytic-like population is responsible for the immune suppression mediated by myeloid-derived suppressor cells. *Blood.* 2011;118:2254–2265. doi:10.1182/blood-2010-12-325753.
 39. Mundy-Bosse BL, Young GS, Bauer T, Binkley E, Bloomston M, Bill MA, Bekaii-Saab T, Carson WE 3rd, Lesinski GB. Distinct myeloid suppressor cell subsets correlate with plasma IL-6 and IL-10 and reduced interferon-alpha signaling in CD4⁺ T cells from patients with GI malignancy. *Cancer Immunol Immunother.* 2011;60:1269–1279. doi:10.1007/s00262-011-1029-z.
 40. Poschke I, Mao Y, Adamson L, Salazar-Onfray F, Masucci G, Kiessling R. Myeloid-derived suppressor cells impair the quality of dendritic cell vaccines. *Cancer Immunol Immunother.* 2012;61:827–838. doi:10.1007/s00262-011-1143-y.
 41. Filipazzi P, Valenti R, Huber V, Pilla L, Canese P, Iero M, Castelli C, Mariani L, Parmiani G, Rivoltini L. Identification of a new subset of myeloid suppressor cells in peripheral blood of melanoma patients with modulation by a granulocyte-macrophage colony-stimulation factor-based antitumor vaccine. *J Clin Oncol.* 2007;25:2546–2553. doi:10.1200/JCO.2006.08.5829.
 42. Mandruzzato S, Solito S, Falisi E, Francescato S, Chiarion-Sileni V, Mocellin S, Zanon A, Rossi CR, Nitti D, Bronte V, et al. IL4Ralpha+ myeloid-derived suppressor cell expansion in cancer patients. *J Immunol.* 2009;182:6562–6568. doi:10.4049/jimmunol.0803831.
 43. Schilling B, Sucker A, Griewank K, Zhao F, Weide B, Görgens A, Giebel B, Schadendorf D, Paschen A. Vemurafenib reverses immunosuppression by myeloid-derived suppressor cells. *Int J Cancer.* 2013;133:1653–1663. doi:10.1002/ijc.28168.
 44. Umansky V, Sevko A, Gebhardt C, Utikal J. Myeloid-derived suppressor cells in malignant melanoma. *J Dtsch Dermatol Ges.* 2014;12:1021–1027. doi:10.1111/ddg.12411.
 45. Rudolph BM, Loquai C, Gerwe A, Bacher N, Steinbrink K, Grabbe S, Tuettgenberg A. Increased frequencies of CD11b(+) CD33(+) CD14(+) HLA-DR(low) myeloid-derived suppressor cells are an early event in melanoma patients. *Exp Dermatol.* 2014;23:202–204. doi:10.1111/exd.12336.
 46. Jordan KR, Amaria RN, Ramirez O, Callihan EB, Gao D, Borakove M, Manthey E, Borges VF, McCarter MD. Myeloid-derived suppressor cells are associated with disease progression and decreased overall survival in advanced-stage melanoma patients. *Cancer Immunol Immunother.* 2013;62:1711–1722. doi:10.1007/s00262-013-1475-x.
 47. Chevolet I, Speckaert R, Schreuer M, Neyns B, Krysko O, Bachert C, Van Gele M, Van Geel N, Brochez L. Clinical significance of plasmacytoid dendritic cells and myeloid-derived suppressor cells in melanoma. *J Transl Med.* 2015;13:9. doi:10.1186/s12967-014-0376-x.
 48. Antonia SJ, Mirza N, Fricke I, Chiappori A, Thompson P, Williams N, Bepler G, Simon G, Janssen W, Lee J-H, et al. Combination of p53 cancer vaccine with chemotherapy in patients with extensive stage small cell lung cancer. *Clin Cancer Res.* 2006;12:878–887. doi:10.1158/1078-0432.CCR-05-2013.
 49. Iclozan C, Antonia S, Chiappori A, Chen DT, Gabrilovich D. Therapeutic regulation of myeloid-derived suppressor cells and immune response to cancer vaccine in patients with extensive stage small cell lung cancer. *Cancer Immunol Immunother.* 2013;62:909–918. doi:10.1007/s00262-013-1396-8.
 50. Ramachandran H, Laux J, Moldovan I, Caspell R, Lehmann PV, Subbramanian RA. Optimal thawing of cryopreserved peripheral blood mononuclear cells for use in high-throughput human immune monitoring studies. *Cells.* 2012;1(3):313–324. doi:10.3390/cells1030313.